

Cycle and flow trusses in directed networks

Taro Takaguchi^{1,2,†}, Yuichi Yoshida^{1,3,‡}

¹ National Institute of Informatics,
2-1-2 Hitotsubashi, Chiyoda-ku, 101-8430 Tokyo, Japan

² JST, ERATO, Kawarabayashi Large Graph Project,
2-1-2 Hitotsubashi, Chiyoda-ku, 101-8430 Tokyo, Japan

³ Preferred Infrastructure, Inc.,
2-40-1 Hongo, Bunkyo-ku, 113-0033 Tokyo, Japan

[†] t_takaguchi@nii.ac.jp

[‡] yyoshida@nii.ac.jp

June 19, 2022

Abstract

When we represent real-world systems as networks, the directions of links often convey valuable information. Finding module structures that respect link directions is one of the most important tasks for analyzing directed networks. Although many methods have been proposed, no consensus on the notion of a directed module has been reached. This lack of consensus results partly because there might exist distinct types of modules in a single directed network, whereas most previous studies focused on an independent criterion for modules. To address this issue, we propose a generic method to find the so-called truss structures in directed networks. Our method is able to extract two distinct types of trusses, named the cycle truss and the flow truss, from a unified framework. By applying the method to empirical networks obtained from a wide range of research fields, we find that most real networks contain both cycle and flow trusses. In addition, the abundance of (and the overlap between) the two types of trusses may be useful to characterize module structures in a wide variety of empirical networks. Our findings shed light on the importance of simultaneously considering different types of modules in directed networks.

Introduction

Analysis methods developed in network science provide us with useful tools for investigating and characterizing the kinds of network structures observed in real-world systems [1]. Standard techniques in network science include characterizing global properties of networks, measuring centralities of nodes and links, and classifying nodes into groups [2, 3]. Finding relevant subgroups of nodes, often called communities or modules, is a fundamental problem. This problem is referred to as the community detection problem [4, 5], which has been studied in different disciplines including computer science, statistics, and statistical physics. Although there is no unifying definition of a community, information regarding communities in networks gives us a guide to summarize large-scale networks [6], to predict the existence of links [7], and to reveal functional organization in real networks [8, 9].

Within the community detection problem for real-world networks, the direction of links plays a crucial role. Although the majority of community detection algorithms assume undirected networks as their input, several algorithms are explicitly designed for directed networks. Examples of such algorithms include extensions of spectral partitioning [10, 11], a generalization of the modularity maximization [12], and the map equation [6] (for a comprehensive review see Ref. [13]). These algorithms often successfully detect communities that satisfy their criteria. Nevertheless, it remains an open problem as to how to choose an algorithm when we are given directed network data. For undirected networks, the local density of links within a subgroup of nodes is arguably a suitable criterion for a module, regardless of the details of the algorithms [5]. In contrast, for directed networks, the directionality of links can alter the module structure, even when we observe the same link density in two subgroups of nodes. The choice of algorithms crucially depends on what types of modules we expect to find. In addition, some algorithms are known to fail to detect certain types of module structure [14, 13]; the impact of this drawback is not clear until we analyze the network. Therefore, a generic method to find directed modules is necessary for understanding the nature of module structures in real-world

directed networks.

To address this issue, in this paper, we propose an algorithm for extracting module structures in directed networks. The following observations underlie the core concept of our method. First, there could be different types of modules within a single directed network. For example, one part of a network can be an all-to-all connected module, whereas another part can form a layered structure [13]. Second, it is not necessary to divide the entire network into modules. For example, the World Wide Web network is well known to exhibit the so-called bow-tie structure [15, 16]. This fact implies that the different parts of a directed network may not be regarded as modules to an equal degree. Instead, extraction of modules from the network should be considered. Previous algorithms often ignore these observations: they aim at partitioning the entire network into modules based on a single objective function. Therefore, we develop a method to extract two distinct types of modules, called the cycle truss and the flow truss, using a unified framework. Our method relies on pattern matching and local agglomeration of directed triangles (i.e., connected subgraphs composed of three nodes and three links).

We apply the proposed method to a variety of empirical networks to verify its practicality. First, we observe that the extracted trusses seem to capture meaningful subgroups of nodes in networks with node label data. Second, because our method simultaneously detects the two types of modules, we can use them as features for classifying different networks. Empirical networks obtained from the same categories (e.g., social or biological) tend to show a similar degree of abundance of the two types of trusses. In addition, the overlap between the two types of trusses captures another kind of similarity between networks in a given category. Our findings demonstrate the importance of simultaneously considering different types of modules in directed networks to understand the common properties underlying the organization of modules.

Results

Definitions of cycle and flow trusses

In this paper, we assume that the focal network is directed and simple, i.e., there are no self-loops or multiple links in the same direction. Bidirectional connections between two nodes are possible: links from node i to node j , and from j to i may coexist. We also assume that links are unweighted. First, we define cycle and flow triangles as the elements of cycle and flow trusses, respectively. A cycle triangle is a directed cycle composed of three nodes (see Fig. 1(a)). A flow triangle is a connected subgraph composed of three nodes that have out-degrees equal to zero, one, and two (see Fig. 1(b)). A flow triangle is also called a feed-forward loop [17, 18]. Next, we define the cycle and flow trusses by generalizing the k -truss, originally defined for undirected networks [19]. A cycle (flow) k -truss is a maximal connected subgraph of a network in which every link is involved in at least k cycle (flow) triangles within the subgraph [20] (see Fig. 1(c) for an example). Free parameter k takes a nonnegative integer value and controls the extent to which triangles are overlapped within a truss. It should be noted that a cycle (flow) truss may contain flow (cycle) triangles.

The definitions of the cycle and flow k -trusses satisfy the requirements described in Introduction, as we can see in the example shown in Fig. 1(c). To be more precise, these definitions enable us to find two distinct types of modules using the unified framework. In addition, this method extracts modules from a network, instead of partitioning the entire network into modules. The algorithm for finding cycle and flow k -trusses in a given network is a modified version of that for undirected truss [21]. The details of the algorithm are presented with pseudo-codes in Materials and Methods.

The definitions of the trusses lead to their basic properties as follows: First, there can be multiple cycle (flow) k -trusses in a network. Second, cycle and flow $(k+a)$ -trusses are subgraphs of cycle and flow k -trusses, respectively ($a = 1, 2, \dots$). Third, the node sets of two k -trusses of the same type can overlap, but their link sets must be disjoint if we take into account the

maximal property in the definition. Fourth, the complete graph with k nodes in which all node pairs are connected for both directions is both a cycle $(k - 2)$ -truss and a flow $3(k - 2)$ -truss at the same time ($k \geq 3$).

We assign a link from nodes i to j with the truss number $k_{i \rightarrow j}$ defined by

$$k_{i \rightarrow j} \equiv \max \{k \mid (i \rightarrow j) \in E_k\}, \quad (1)$$

where E_k is the set of links involved in k -trusses. We denote the truss number for cycle and flow trusses by $k_{i \rightarrow j}^c$ and $k_{i \rightarrow j}^f$, respectively. We use the superscripts ‘c’ and ‘f’ to represent the variables related to the cycle and flow trusses throughout this paper. The truss number indicates the extent of agglomeration of triangles around a link. For example, in the network shown in Fig. 1(c), link $(i_1 \rightarrow j_1)$ has $(k^c, k^f) = (2, 0)$ and link $(i_2 \rightarrow j_2)$ has $(k^c, k^f) = (0, 2)$. We are also interested in the maximum values of $k_{i \rightarrow j}^c$ and $k_{i \rightarrow j}^f$ over all the links. We call these values the maximum truss numbers; they are denoted by k_{\max}^c and k_{\max}^f for cycle and flow trusses, respectively. For the network shown in Fig. 1(c), $k_{\max}^c = k_{\max}^f = 2$ holds.

There are several relationships between the cycle and flow trusses and other notions of directed subgraphs presented in previous studies. Detecting directed triangles that are significantly over-presented is a key idea of motif analysis [17, 18]. The original notion of the motif often focuses on subgraphs with a small number of nodes (e.g., three or four). Previous studies [22, 23, 24, 25] considered the generalization of motifs by aggregating the motifs sharing links so as to construct functional modules larger than single motifs. In particular, the generalization of the feed-forward loop motif (called the flow triangle in this paper) described in Refs. [22, 23, 24, 25] is an example of the flow 1-truss in our definition. Another related notion is the directed k -clique [26]. A directed k -clique is a subgraph with k nodes and $k(k - 1)/2$ links, in which the k nodes has a linear ordering and all node have directed links to all the lower-rank nodes. A directed k -clique module is defined by a union of adjacent directed k -cliques. Two directed k -cliques are said to be adjacent if the two have $k - 1$ nodes in common. A directed k -clique module is a flow $(k - 2)$ -truss ($k \geq 3$); however, the converse does not always hold true. Therefore, the cohesiveness of the flow k -trusses is between those of the generalization

of feed-forward loop motif and the directed k -clique modules. A cycle k -truss does not exactly correspond to any of the previous notions. Based on the definition, a cycle truss is a strongly connected component (i.e., any node in the cycle truss is connected to all the other nodes via directed links).

Trusses in empirical networks

We apply the proposed method to empirical network data that are assigned with predefined node labels so as to demonstrate that cycle and flow trusses can extract meaningful modules. We use two networks obtained from different fields: the neural network of *Caenorhabditis elegans* (*C. elegans*) [27] and the network between words collected via word association experiments [28].

Neural network of *Caenorhabditis elegans* The *C. elegans* neural network comprises 279 nodes, which correspond to neurons, and 2,990 links between the nodes. A chemical synapse between two neurons is represented as a directed link and an electrical junction as two directed links in both directions between the node pair [27]. Each neuron is assigned with a unique name and additional information such as soma positions in the worm’s body and functional categories (i.e., sensory neuron, interneuron, or motor neuron), which enables us to interpret the neuronal functions of the extracted trusses.

In Fig. 2, the resulting k -trusses are depicted. We focus on the cycle $k_{\max}^c = 3$ - and flow $k_{\max}^f = 9$ -trusses, which are the most cohesive trusses in the network. In this case, both the cycle 3- and flow 9-trusses are a single weakly connected components (i.e., any pair of nodes in each of the trusses is connected if we discard the link direction). When we map the cycle and flow trusses in the entire network (Fig. 2(a)), neither of these trusses is localized in any particular part of the worm body, but instead, spans almost the entire range of the body (from head to tail). We can see that a small number of nodes bridges most of the triangles in the trusses. The cycle 3-truss (Fig. 2(b)) consists of four command interneurons relevant for locomotion (AVAL, AVAR, AVBR, and PVCR) and three motor neurons in the ventral cord of the worm (VA08,

VA09, and VB09). Here, we follow the description of each neuron in Ref. [29]. These seven neurons in the cycle 3-truss are tightly connected to each other; however, certain node pairs have a link in only one direction. On the other hand, the flow 9-truss (Fig. 2(c)) consists of 13 interneurons relevant to locomotion (AVAL, AVAR, AVBL, AVBR, AVDL, AVDR, AVEL, AVER, AVJL, AVJR, PVCL, PVCR, and SABVR) and seven motor neurons in the dorsal cord of the worm (DA1, DB03 to 06, and DVA), except for that in the ventral cord (AS01). Although we need further explanation by biological experts as to why these neurons constitute the cycle and flow trusses, the trusses seem to represent functional modules of neurons. The cycle and flow trusses overlap with each other and have four command interneurons AVAL, AVAR, AVBR, and PVCR in common. This fact arises logically, as the command interneurons related to locomotion should play a central role in mediating the motor neurons in the ventral and dorsal cords [27]. This example of the *C. elegans* neural network demonstrates the ability of our proposed method to extract different types of cohesive modules from networks. In addition, the overlap between the two types of trusses can shed light on the importance of nodes that bridge different modules.

Word network of the Edinburgh Associative Thesaurus Our second example is the graph representation of the Edinburgh Associative Thesaurus (EAT), which was collected through word association experiments with subjects [28]. A directed link from nodes (i.e., words) i to j represents the associative relationship between the two: for subjects, word j comes to mind when they are shown word i as a stimulus. After the aggregation of the results of word association experiments for many subjects with different stimuli, the EAT network contains 23,219 nodes and 325,029 links between them.

In Fig. 3, the resulting k -trusses are depicted. We show the cycle $k_{\max}^c = 2$ - and flow $k_{\max}^f = 8$ -trusses. Unlike the results of the *C. elegans* neural network (Fig. 2), there are multiple disjoint cycle and flow trusses with $k_{\max}^c = 2$ and $k_{\max}^f = 8$. We can see that each of the trusses consists of words related to a topic, for example, religion, emotion, health, and

poem. All six of the cycle 2-trusses composed of five nodes are fully connected, in which all node pairs have links in both directions. Each of the cycle 2-trusses related to emotion, health, and color strongly overlap with one of the flow 8-trusses (Fig. 3). Only the flow 8-truss related to liquor, the largest one, is less overlapped with the cycle trusses than the other flow 8-trusses are. We can interpret the difference between the cycle and flow trusses as follows. The words constituting a cycle truss have an equal relationship with each other such that the experimental subjects tend to recall all words based on each word. By contrast, the words constituting a flow truss have a hierarchical relationship such that some words remind the subjects of other words but the converse rarely occurs. If we discard the link direction, we cannot distinguish the modules of the cycle and flow trusses. Therefore, this example demonstrates that the link direction plays an important role in finding modules; our method successfully takes into account the link direction.

Basic statistics of trusses in various networks The basic statistics of the truss structure for empirical networks obtained from 12 different fields are summarized in Tables. S1 and S2 of Supplementary Materials (SM). Except for k_{\max}^f for the circuit networks and a few examples, almost all k_{\max}^c and k_{\max}^f are nontrivial. Additionally, the k_{\max}^c and k_{\max}^f values do not necessarily increase with the number of cycle and flow triangles. This result implies that the trusses can retain the information regarding the module structure, irrespective of the count of these triangles.

Classification of networks based on truss number distributions

We can use the truss number statistics to classify various networks. Intuitively, a network is more cycle (flow) truss oriented if the links tend to have larger cycle (flow) truss numbers. Note that a large truss number implies the agglomeration (and abundance) of triangles. To quantify how much a network is truss oriented, we define a measure D as

$$D \equiv \frac{1}{K} \sum_{k=0}^K (F_{\text{rand}}(k) - F_{\text{orig}}(k)), \quad (2)$$

where $F(k)$ is the complementary cumulative distribution of truss numbers defined by $F(k) \equiv \sum_{k'=0}^k f(k')$ and $f(k')$ (in the sum) is the frequency distribution of the truss number. In Eq. 2, the subscripts “orig” and “rand” represent the distributions for the original and randomized networks, respectively. We randomize the original network by rewiring links in a uniformly random manner while retaining the in- and out-degrees of all nodes. The range of the sum over k is determined by K . Here, we choose $K \equiv \min \{k \mid F_{\text{orig}}(k) > 0.9 \wedge F_{\text{rand}}(k) > 0.9\}$. We do not assume $K = k_{\text{max}}$, because k_{max} might be sensitive to noise in the network data. The measure D takes a value in $[-1, 1]$; a large positive value of D represents that the links in the original network tend to have a larger truss number than those in the randomized networks. We denote the measure D for the cycle and flow truss numbers by D^c and D^f , respectively. In Figs. 4(a) and 4(b), we plot the truss number distributions $f^c(k)$ and $f^f(k)$ of the *C. elegans* neural network and the randomized networks. The k_{max}^c and k_{max}^f values are larger for the original network than those for the randomized networks. The proportions of links with large k values are also larger for the original than the randomized networks. For this network, we obtain $(D^c, D^f) = (0.122, 0.329)$. Therefore, the *C. elegans* network is inclined to have more flow trusses than cycle trusses, which agrees well with our intuition based on Figs. 4(a) and 4(b).

The measure D allows us to compare various networks of different sizes in terms of truss tendency. In Fig. 4(c), we show the scatter plot of D^c and D^f for the empirical networks. As we can see, the networks of certain categories such as airport, circuit, citation, and food webs loosely fall into the similar positions on the plane. The points are located around the diagonal because networks with larger numbers of triangles tend to have larger D values. This phenomenon occurs because our randomization procedure does not conserve the number of triangles in the original network; the randomization tends to destroy triangles, and consequently, destroy the truss structure. This reasoning is supported by the observation shown in Fig. S1 in SM. The elements of the first principle component of the plot shown in Fig. 4 exhibit a strong positive correlation with the clustering coefficient [30] after discarding the link directions. Nevertheless,

Fig. 4 provides the information regarding network topology beyond simply the count of the triangles. For example, there are several distinguishable classes of network (such as citation and circuit networks) in which either cycle or flow trusses are dominant. The neural, airport, and web networks contain both types of trusses. The metabolic networks [31] tend to have few cycle or flow trusses as comparable with those in the randomized networks. These observations suggest the usefulness of the cycle and flow trusses to characterize different types of directed networks.

Overlap between cycle and flow trusses

In the previous section, we separately considered the properties related to the cycle and flow trusses. As we observed in the example networks (Figs. 2 and 3), the overlap between the two types of trusses can be another characteristic of the networks. In particular, we are interested in the overlap between highly cohesive cycle and flow trusses with large k values. To analyze the overlap, we plot the joint frequency distribution of truss numbers (k^c, k^f) for four example networks, i.e., the *C. elegans* neural network, the EAT network, the USairport 2010 network [32], and the web-Google network [33] (Fig. 5). In these plots, a cell at (k^c, k^f) indicates the proportion of links with these truss numbers. The plots of (k^c, k^f) frequencies indicate the unique characteristics of the different networks. In the *C. elegans* neural network (Fig. 5(a)), the links with $k^c = 3$ have only $7 \leq k^f \leq 9 = k_{\max}^f$. This property suggests that the size of the cycle k_{\max}^c -truss is smaller than that of the flow k_{\max}^f -truss and a large section of the cycle truss overlaps with the flow truss, as we observed in Fig. 2. By contrast, for the EAT network (Fig. 5(b)), the majority of links have relatively small truss numbers, as $k^c = 0$ and $0 \leq k^f \leq 3$. Thus, the cohesive cycle and flow trusses are not strongly overlapped. The plots for the USairport 2010 (Fig. 5(c)) and web-Google (Fig. 5(d)) networks look similar, such that we can see the colored cells along the diagonal of slope equal to 3. This observation suggests that in these networks there are complete subgraphs within which node pairs are connected in both directions. This situation may correspond to airports within local regions and web pages

under the same directories.

To quantify the overlap between the cohesive cycle and flow trusses in a network, we define

$$R \equiv \frac{|\{e \in E \mid (k_e^c > k_{\text{med}}^c) \wedge (k_e^f > k_{\text{med}}^f)\}|}{|\{e \in E \mid (k_e^c > k_{\text{med}}^c) \vee (k_e^f > k_{\text{med}}^f)\}|}, \quad (3)$$

where E is the set of all links and k_{med}^c and k_{med}^f are the median values of $f^c(k)$ and $f^f(k)$ (indicated by the dashed lines in Fig. 5), respectively. The measure R characterizes the proportion of links with large k^c and k^f values among those with large k^c or k^f values. The measure R takes a value in $[0, 1]$; a large R value indicates a strong overlap between the cohesive cycle and flow trusses. For the four networks shown in Fig. 5, we obtain $R = 0.531$, 0.383 , 0.983 , and 0.540 for the *C. elegans* neural network, the EAT network, the USairport 2010 network, and the web-Google network, respectively.

In Fig. 6, we plot the R values for the empirical networks (i.e., the same set that we used in Fig. 4, except for the metabolic networks). First, we can see that the networks of some categories have the R values close to the extreme cases, i.e., 0 or 1. For the airport networks, the R values for the three networks are almost equal to unity. This result follows logically, because almost all of the adjacent pairs of nodes have bidirectional links (Table S1 in SM). Therefore, any triplet of nodes is likely to constitute a cycle triangle if it composes a flow triangle and vice versa. For the circuit, citation, gene regulatory, P2P, and software networks, the R values are close to zero, because these types of networks have huge gaps between the number of cycle and flow triangles (Table S1). The three circuit networks do not contain any flow triangles. For the citation, gene regulatory, P2P, and software networks, the number of cycle triangles is much smaller than that of flow triangles.

The following, neural, web, and word networks tend to have R values greater than 0.5, although fluctuations within a category are large. The food webs tend to have R values less than 0.5. The results for the metabolic networks are shown in Fig. S2 in SM; the majority of these networks have R values of 0.491 ± 0.0481 (mean \pm standard deviation). These observations may indicate the usefulness of the R value to characterize the tendency of module organization

for different categories of networks.

Discussion

In this paper, we proposed the cycle and flow k -trusses in order to extract two distinct types of cohesive modules from directed networks. We developed an efficient algorithm for computing these trusses and defined the measures used to quantify the module organization in a network based on the truss properties. Applications of our method to a wide variety of empirical networks illustrated that most empirical networks contain either type of trusses or both of them. We investigated the extracted trusses for several networks with the given node labels and found that the trusses seem to capture relevant subgroups of nodes. We also found that the abundance of (and the overlap between) cycle and flow trusses helps us to classify empirical networks obtained from different fields. These findings suggest the importance of exploring different types of modules in directed networks. We believe that our method will be a useful tool for investigating module structure in directed networks.

Our method assumes that the focal network is directed and unweighted. However, the importance of link weight in many systems has been suggested in previous work (e.g., Ref. [34]). This point is a clear limitation of the present method and a suitable generalization for weighted networks is warranted. Although we determined the existence of truss structures in empirical networks, the origins and functional roles of these trusses are not yet well understood. Dynamical models of the growth processes of directed networks that yield truss structures will be potential future work, providing fully understanding of the organization of modules in directed networks.

Materials and Methods

Data

The network data sets used in the present study were downloaded from the following websites.

- The airport, communication, following, and software networks: <http://konect.uni-koblenz.de/>
- the USairport500 network: <http://toreopsahl.com/datasets/#usairports>
- The circuit networks and the word networks: <http://www.weizmann.ac.il/mcb/UriAlon/download/collection-complex-networks>
- The allcites network (the U.S. supreme court citation network): <http://fowler.ucsd.edu/judicial.htm>
- The cit-HepPh, cit-HepTh, social, slashdot-0902, twitter.combined, wiki-Vote, P2P, and the web networks: <http://snap.stanford.edu/data/>
- The food webs and the Edinburgh Associative Thesaurus: <http://vlado.fmf.uni-lj.si/pub/networks/data/>
- The gene regulatory networks; <http://info.gersteinlab.org/Hierarchy>
- The *C. elegans* neural network: <http://www.wormatlas.org/neuronalwiring.html>
- The brain connectivity networks: <https://sites.google.com/site/bctnet/datasets>
- The mac95 network: http://www.biological-networks.org/?page_id=25
- The polblog network (the hyperlink network between weblogs on US politics): <http://www-personal.umich.edu/~mejn/netdata/>

The metabolic networks were based on those used in Ref. [31] and the network data were given by Kazuhiro Takemoto through personal communication. Any additional information from links, such as the weight, sign, or time stamp, were discarded from the network data. We also removed the self-loops and multiple links to make the networks simple.

Algorithms to compute trusses

We describe our algorithm for finding the flow and cycle k -trusses in a network. For a network G , the sets of nodes and links are denoted by $V(G)$ and $E(G)$, respectively. For a node $v \in V(G)$, we define $N_G^+(v)$ as the set of out-neighbors of v , that is, $N_G^+(v) = \{w \in V(G) \mid vw \in E(G)\}$; we define $\text{deg}_G^+(v)$ as the out-degree of v , i.e., $\text{deg}_G^+(v) = |N_G^+(v)|$. Here, for the sake of simplicity, we denote the link from node u to node v by uv .

Our algorithm uses a subroutine called COMMONNEIGHBOR (Algorithm 1). This subroutine takes two networks G and G' on the same node set V and two nodes $u, v \in V$, and returns the set of nodes w such that $uw \in E(G)$ and $vw \in E(G')$. This subroutine will be used to enumerate

the cycle or flow triangles involving the link uv . The algorithm is relatively straightforward: it chooses either u or v , enumerates its out-neighbors w , and then checks whether w is also an out-neighbor of the other unchosen node. For efficiency, we choose u if $\deg_G^+(u) < \deg_{G'}^+(v)$ and choose v otherwise. Using hash tables for storing out-neighbors of nodes, the time complexity of COMMONNEIGHBOR is bounded by $O(\min\{\deg_G^+(u), \deg_{G'}^+(v)\})$.

Now we present our algorithm for enumerating cycle trusses (Algorithm 2). Given a network G , it computes cycle k -trusses for all k at once.

First, for every link $uv \in E(G)$, we count the number of cycle triangles involving uv and store the number to $c[uv]$ (Line 6). This can be done by calling COMMONNEIGHBOR(G', G, u, v), where G' is the network obtained from G by reversing the directions of links. This is because if there exists a cycle triangle in G with links uv, vw , and wu , then G' contains the link uw and G contains the link vw .

Next, starting with $k = 0$, as long as the links remain, we perform the following process: As long as there is a link uv such that $c[uv]$ is at most k , we set the truss number $\ell[uv]$ of uv to be k (Line 11), then for each cycle triangle involving the link uv , we decrease the count of the other two links (Line 12-14), and finally Finally, we remove the link uv from the network (Line 15). If there is no link with a count of at most k , we increment the value of k and repeat the process. Note that, when the process starts for a particular value of k , all links have counts of at least k , and thus, all these links have truss numbers of at least k . On the other hand, when we remove a link in the process for a particular k value, because we have only removed links that cannot be a member of a cycle $(k+1)$ -truss, its truss number is at most k . Therefore, each link is assigned with the correct truss number.

The overall time complexity of CYCLETRUSS is dominated by the time complexity of enumerating the cycle triangles. Naively, this can be bounded by

$$\sum_{uv \in E(G)} \deg_G^+(v) = \sum_{v \in V(G)} \deg_G^+(v)^2 = O\left(N^2 \cdot \frac{M}{N}\right) = O(NM),$$

where N and M are the number of nodes and links, respectively, in the input network. In

practice, however, the time taken runs is almost linear with M for real networks.

Finally, we explain our algorithm for enumerating flow trusses (Algorithm 3), which simultaneously computes flow k -trusses for all k values. Conceptually, FLOWTRUSS is almost the same as CYCLETRUSS. However, for a link uv and a node w , there are three types of a flow triangle involved: (i) a flow truss with links uv , wv , and uw , (ii) a flow truss with links uv , wv , and wu , and (iii) a flow truss with links uv , vw , and wu . These links can be enumerated by calling COMMONNEIGHBOR(G, G'), COMMONNEIGHBOR(G', G'), and COMMONNEIGHBOR(G, G'), respectively, where G' is the network obtained from G by reversing the directions of all links. The other parts of the algorithm and the analysis of time complexity are the same as those of CYCLETRUSS, and therefore we omit them.

References and Notes

- [1] M. E. J. Newman. *Networks: An Introduction*. (Oxford University Press, Oxford, 2010).
- [2] L. da F. Costa, F. A. Rodrigues, G. Travieso, P. R. Villas Boas. Characterization of complex networks: A survey of measurements. *Adv. Phys.* **56**, 167–242 (2007).
- [3] A. Barrat, M. Barthélemy, A. Vespignani. *Dynamical Processes on Complex Networks*. (Cambridge University Press, Cambridge, 2008).
- [4] M. A. Porter, J.-P. Onnela, P. J. Mucha. Communities in Networks. *Not. Am. Math. Soc.* **56**, 1082–1097 (2009).
- [5] S. Fortunato. Community detection in graphs. *Phys. Rep.* **486**, 75–174 (2010).
- [6] M. Rosvall, C. T. Bergstrom. Maps of random walks on complex networks reveal community structure. *Proc. Natl. Acad. Sci. U.S.A.* **105**, 1118–1123 (2008).
- [7] A. Clauset, C. Moore, M. E. J. Newman. Hierarchical structure and the prediction of missing links in networks. *Nature* **453**, 98–101 (2008).

- [8] J. Chen, B. Yuan. Detecting functional modules in the yeast protein-protein interaction network. *Bioinformatics*, 22(18):2283–2290, 2006.
- [9] Y. Sohn, M.-K. Choi, Y.-Y. Ahn, J. Lee, J. Jeong. Topological cluster analysis reveals the systemic organization of the *Caenorhabditis elegans* connectome. *PLOS Comput. Biol.* **7**, e1001139 (2011).
- [10] F. Chung. Laplacians and the Cheeger inequality for directed graphs. *Ann. Comb.* **9**, 1–19 (2005).
- [11] Y. Yoshida. Nonlinear Laplacian for digraphs and its applications to network analysis. *Proceedings of the Ninth ACM International Conference on Web Search and Data Mining*, San Francisco, CA, USA, 22 to 25 February 2016, pp. 483–492.
- [12] E. A. Leicht, M. E. J. Newman. Community structure in directed networks. *Phys. Rev. Lett.* **100**, 118703 (2008).
- [13] F. D. Malliaros, M. Vazirgiannis. Clustering and community detection in directed networks: A survey. *Phys. Rep.* **533**, 95–142 (2013).
- [14] Y. Kim, S.-W. Son, H. Jeong. Finding communities in directed networks. *Phys. Rev. E* **81**, 016103 (2010).
- [15] A. Broder, R. Kumar, F. Maghoul, P. Raghavan, S. Rajagopalan, R. Stata, A. Tomkins, J. Wiener. Graph structure in the Web. *Comput. Networks* **33**, 309–320 (2000).
- [16] B. Corominas-Murtra, J. Goñi, R. V. Solé, C. Rodríguez-Caso. On the origins of hierarchy in complex networks. *Proc. Natl. Acad. Sci. U.S.A.* **110**, 13316–13321 (2013).
- [17] R. Milo, S. Shen-Orr, S. Itzkovitz, N. Kashtan, D. Chklovskii, U. Alon. Network motifs: simple building blocks of complex networks. *Science (New York, N.Y.)* **298**, 824–827 (2002).

- [18] U. Alon. Network motifs: theory and experimental approaches. *Nat. Rev. Genet.* **8**, 450–461 (2007).
- [19] J. Cohen. Trusses : Cohesive Subgraphs for Social Network Analysis. Technical report (National Security Agency, Fort Meade, MD, 2008).
- [20] In the original definition for undirected networks [19], the k -truss is the maximal subgraph in which every link is involved in $(k-2)$ triangles, not k triangles. We modify the definition in order to make the truss number of links involved in no triangles zero.
- [21] J. Wang, J. Cheng. Truss decomposition in massive networks. *Proc. VLDB Endowment* **5**, 812–823 (2012).
- [22] R. Dobrin, Q. K. Beg, A.-L. Barabási, Z. N. Oltvai. Aggregation of topological motifs in the Escherichia coli transcriptional regulatory network. *BMC Bioinform.* **5**, 10 (2004).
- [23] N. Kashtan, S. Itzkovitz, R. Milo, and U. Alon. Topological generalizations of network motifs. *Phys. Rev. E* **70**, 031909 (2004).
- [24] L. V. Zhang, O. D. King, S. L. Wong, D. S. Goldberg, A. H. Y. Tong, G. Lesage, B. Andrews, H. Bussey, C. Boone, F. P. Roth. Motifs, themes and thematic maps of an integrated Saccharomyces cerevisiae interaction network. *J. Biol.* **4**, 6 (2005).
- [25] T. Michoel, A. Joshi, B. Nachtergaele, Y. Van de Peer. Enrichment and aggregation of topological motifs are independent organizational principles of integrated interaction networks. *Mol. Biosyst.* **7**, 2769–2778 (2011).
- [26] G. Palla, I. J. Farkas, P. Pollner, I. Derényi, T. Vicsek. Directed network modules. *New J. Phys.* **9**, 186 (2007).
- [27] L. R. Varshney, B. L. Chen, E. Paniagua, D. H. Hall, D. B. Chklovskii. Structural properties of the Caenorhabditis elegans neuronal network. *PLOS Comput. Biol.* **7**, e1001066 (2011).

- [28] G. R. Kiss, C. Armstrong, R. Milroy, J. Piper. An associative thesaurus of English and its computer analysis. In *The computer and literary studies*, A.J. Aitken, R.W. Bailey, N. Hamilton-Smith, Eds. (Edinburgh University Press, 1973), pp. 153–165.
- [29] Z.F. Altun, D. H. Hall. Nervous system, general description, In *WormAtlas*, <http://dx.doi.org/doi:10.3908/wormatlas.1.18> (Date accessed: 1st March 2016).
- [30] D. J. Watts, S. H. Strogatz. Collective dynamics of ‘small-world’ networks. *Nature* **393**, 440–442 (1998).
- [31] K. Takemoto. Metabolic networks are almost nonfractal: A comprehensive evaluation. *Phys. Rev. E* **90**, 022802 (2014).
- [32] Tore Opsahl. Why Anchorage is not (that) important: Binary ties and Sample selection, <http://toreopsahl.com/2011/08/12/why-anchorage-is-not-that-important-binary-ties-and-sample-selection/> (Date accessed: 1st March 2016).
- [33] J. Leskovec, K.J. Lang, A. Dasgupta, M.W. Mahoney. Community structure in large networks: Natural cluster sizes and the absence of large well-defined clusters. *Internet Math.* **6**, 29–123 (2009).
- [34] A. Barrat, M. Barthélemy, R. Pastor-Satorras, A. Vespignani. The architecture of complex weighted networks. *Proc. Natl. Acad. Sci. U.S.A.* **101**, 3747–3752 (2004).

Acknowledgments

The authors thank Naoki Masuda for insightful comments. **Author contributions:** T.T. and Y.Y. conceived and designed the research. Y.Y. performed the coding. T.T. and Y.Y. analyzed the data, discussed the results, and wrote the manuscript. **Competing interests:** The authors declare no competing financial interests. **Funding:** Y.Y. acknowledges the financial support

through JST, ERATO, Kawarabayashi Large Graph Project, JSPS Grant-in-Aid for Young Scientists (B) (No. 26730009), and MEXT Grant-in-Aid for Scientific Research on Innovative Areas (No. 24106003).

Supplementary Materials

- Fig. S1. Scatter plot of the first principal component of (D^c, D^f) and the clustering coefficient.
- Fig. S2. Histogram of the R measure for the metabolic networks.
- Tables. S1 and. S2. Statistics of the empirical networks.

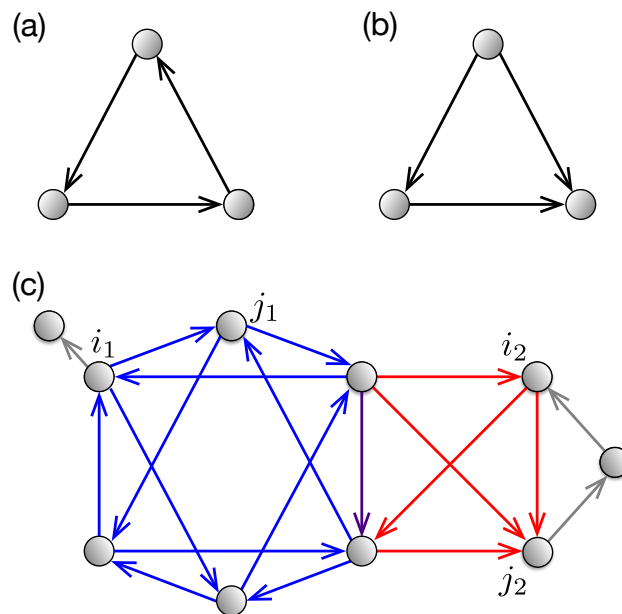


Figure 1: **Definitions of cycle and flow trusses.** (a) a cycle and (b) flow triangles. (c) the cycle (blue) and flow (red) $k = 2$ -trusses in an example network. The vertical arrow colored with purple at the center represents the link that belongs to both of the cycle and flow 2-trusses.

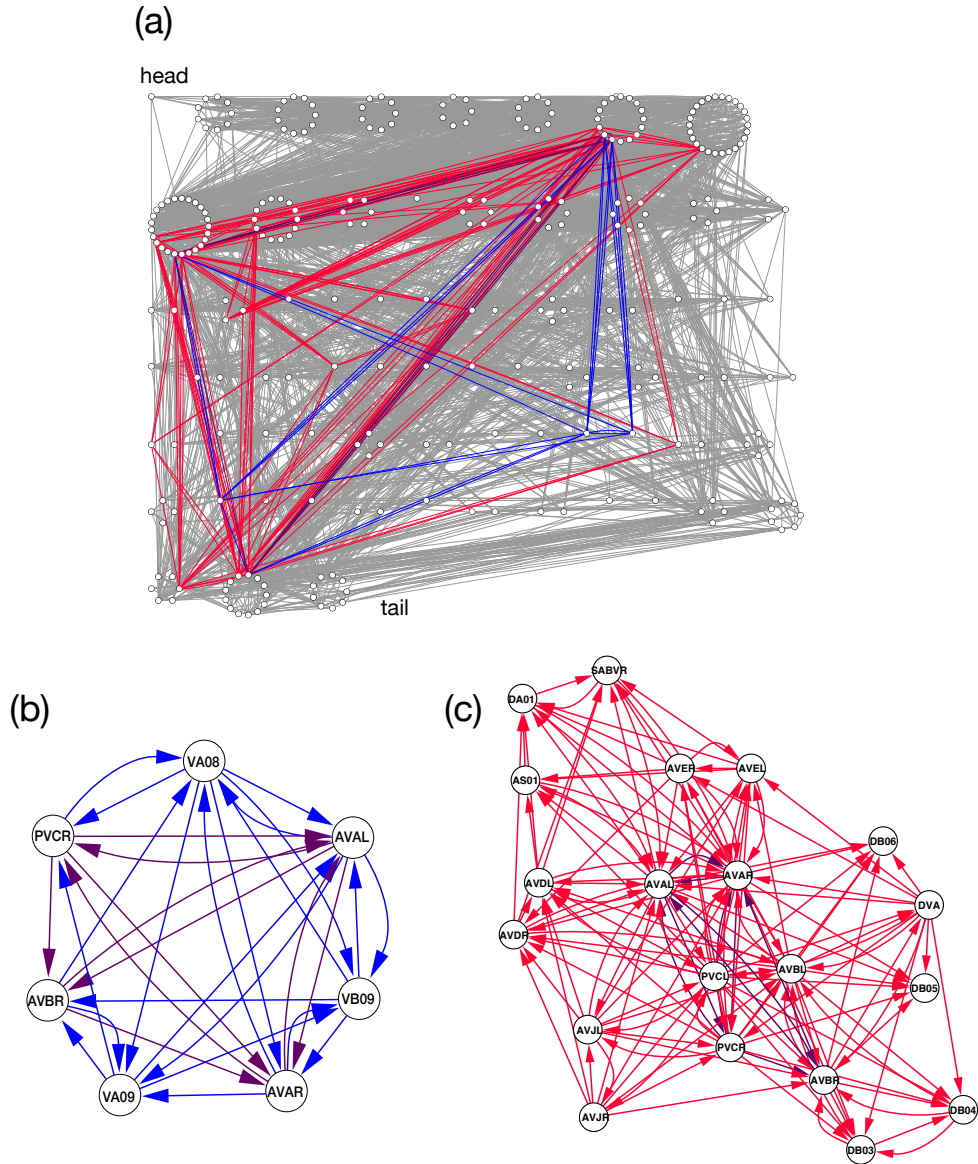


Figure 2: **Cycle and flow trusses in the *C. elegans* neural network.** We set k to $k_{\max}^c = 3$ and $k_{\max}^f = 9$ for the cycle and flow trusses, respectively. The links are colored with blue (in the cycle 3-truss), red (in the flow 9-truss), purple (in both), and gray (remainder). (a) The whole picture of the *C. elegans* neural network. The nodes are ordered according to the soma position in the worm body (head to tail from left to right and from top to bottom). A group of nodes composing a circle have the same position. (b) the cycle 3- and (c) the flow 9-trusses. The node labels indicate the names of neurons.

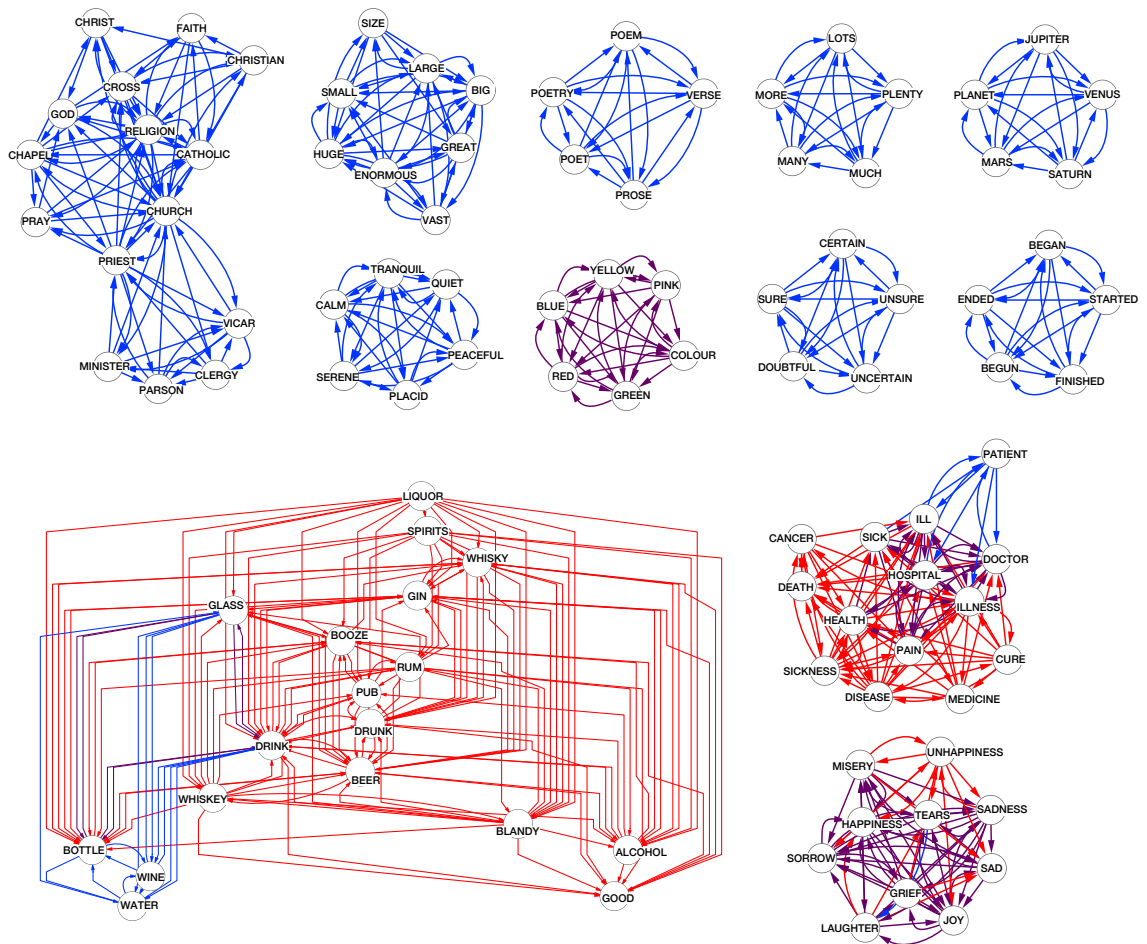


Figure 3: **Cycle and flow trusses in the EAT network.** We set k to $k_{\max}^c = 2$ and $k_{\max}^f = 8$ for the cycle and flow trusses, respectively. The links are colored with blue (in the cycle 2-trusses), red (in the flow 8-trusses), and purple (in both). The node labels indicate the corresponding words.

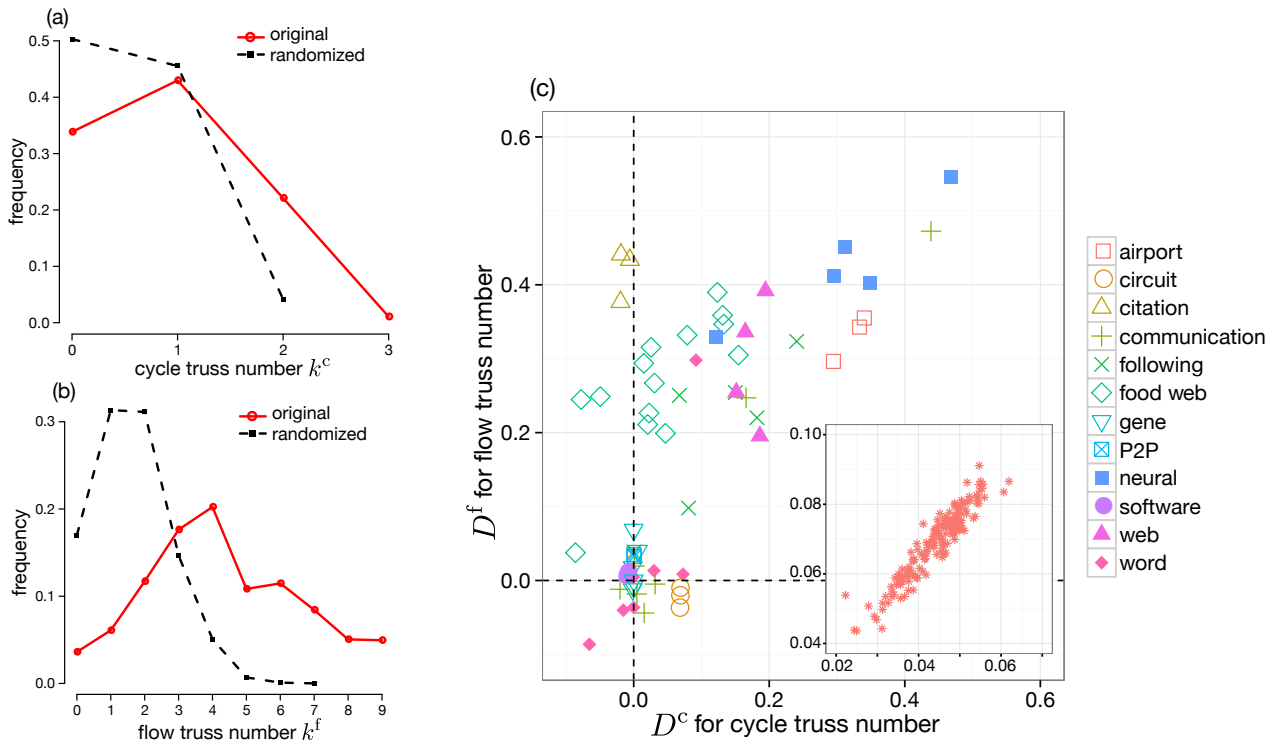


Figure 4: **Distributions of the truss numbers and the D measure.** Distributions of (a) k^c and (b) k^f for the original network and 100 randomized networks of the *C. elegans* neural network. (c) Scatter plot of D^c and D^f for (main panel) empirical networks of the 12 categories and for (inset) the metabolic networks.

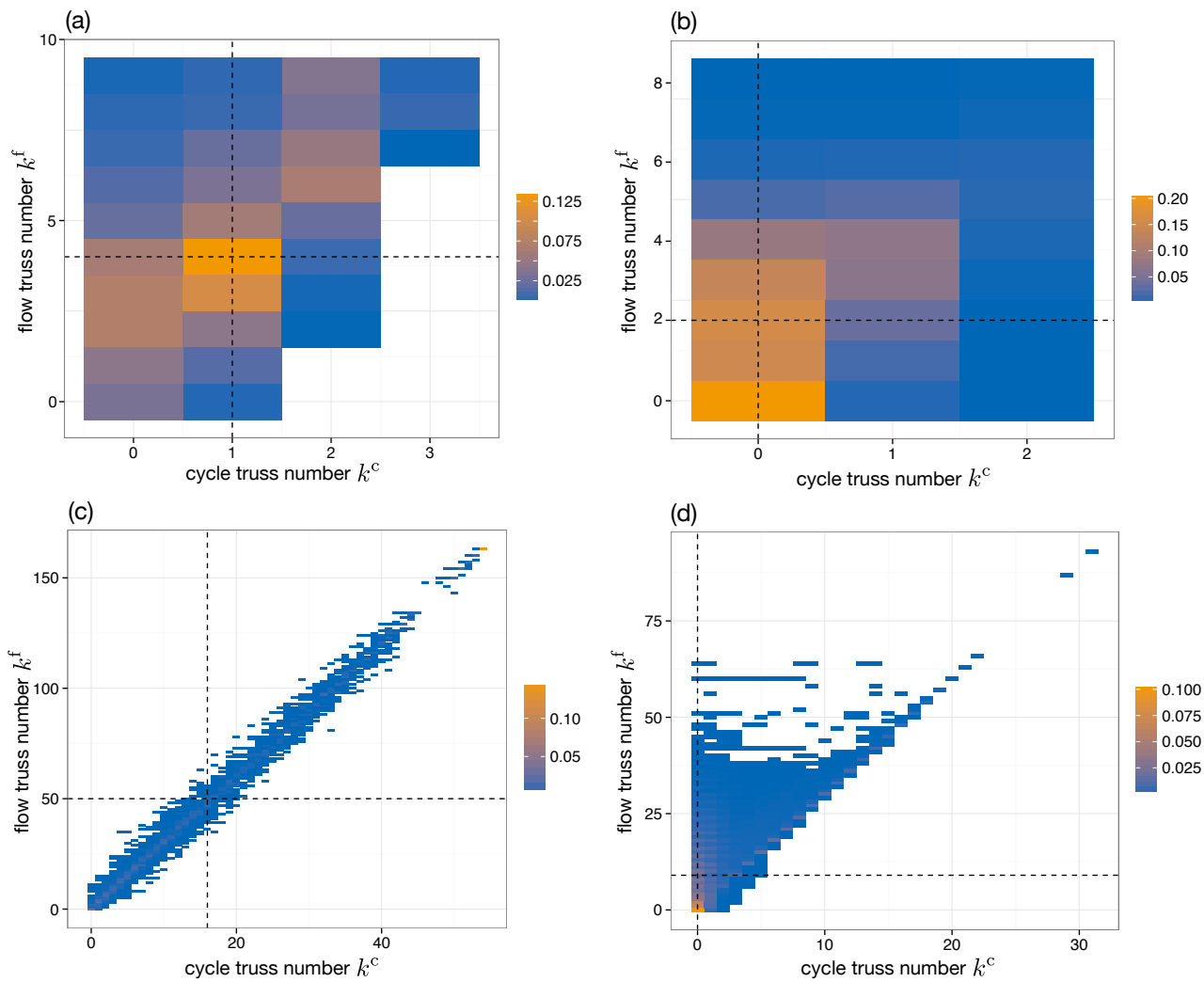


Figure 5: **Joint frequency distribution of (k^c, k^f) .** (a) the *C. elegans* neural network. (b) the EAT network. (c) the USairport 2010 network. (d) the web-Google network. The vertical and horizontal dashed lines indicate the k values that gives the median value for k^c and k^f , respectively.

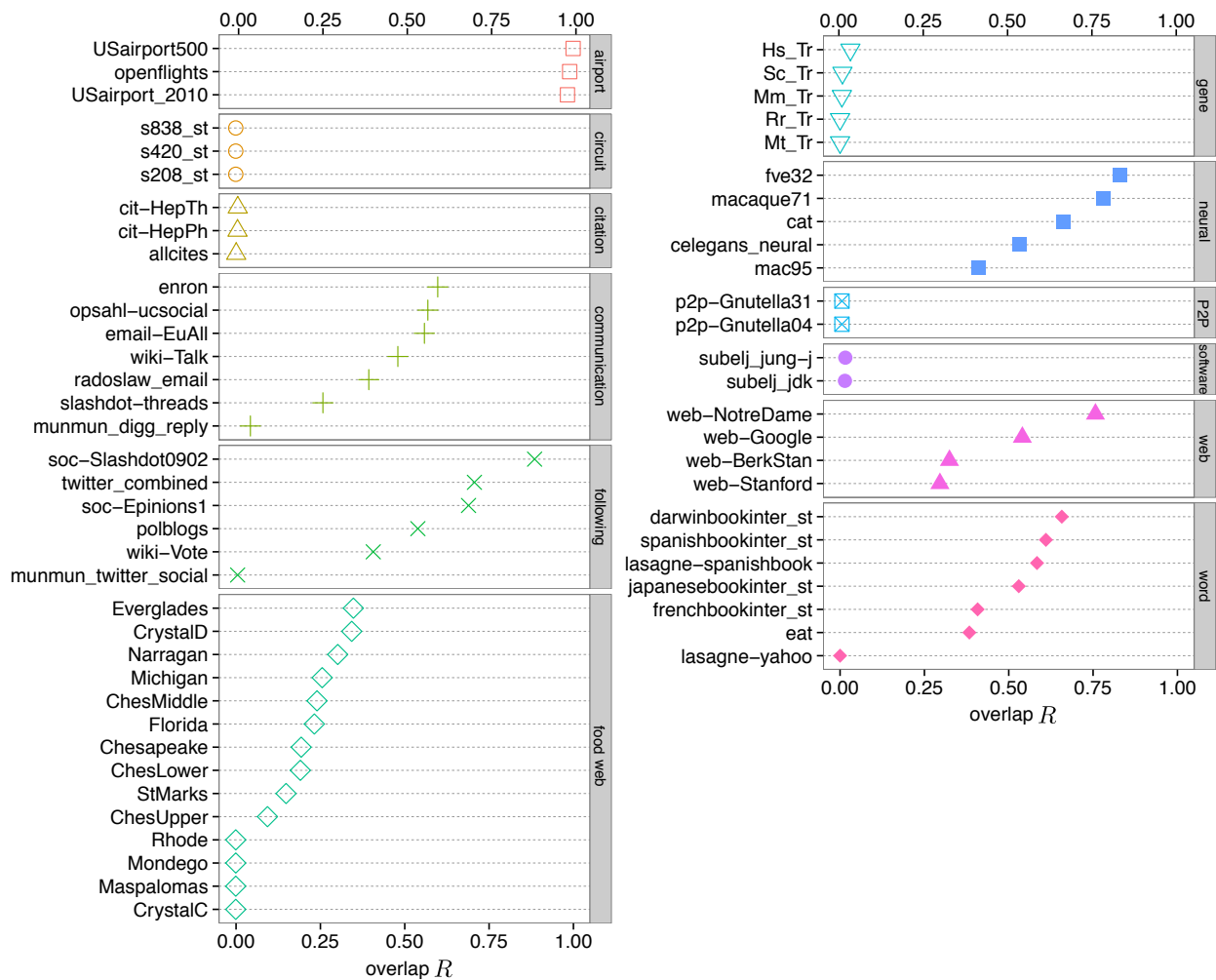


Figure 6: **Overlap measure R for various networks.** The set of empirical networks considered is the same as that used in the main panel of Fig. 4(c).

Algorithm 1

1: **procedure** COMMONNEIGHBOR(G, G', u, v) \triangleright Find all w such that $uw \in E(G)$ and
 $vw \in E(G')$
2: $W \leftarrow \emptyset$.
3: **if** $\deg_G^+(u) < \deg_{G'}^+(v)$ **then**
4: **for** $w \in N_G^+(u) \setminus \{v\}$ **do**
5: **if** $vw \in E(G')$ **then**
6: $W \leftarrow W \cup \{w\}$.
7: **end if**
8: **end for**
9: **else**
10: **for** $w \in N_{G'}^+(v) \setminus \{u\}$ **do**
11: **if** $uw \in E(G)$ **then**
12: $W \leftarrow W \cup \{w\}$.
13: **end if**
14: **end for**
15: **end if**
16: **return** W .
17: **end procedure**

Algorithm 2

```
1: procedure CYCLETRUSS( $G$ ) ▷ Find cycle-trusses in  $G$ 
2:   Let  $G'$  be the network obtained from  $G$  by reversing the directions of links.
3:    $c[e] \leftarrow 0$  for each  $e \in E(G)$ .
4:    $\ell[e] \leftarrow \infty$  for each  $e \in E(G)$ .
5:   for  $uv \in E(G)$  do
6:      $c[uv] \leftarrow |\text{COMMONNEIGHBOR}(G', G, u, v)|$ . ▷ Count cycle triangles involving  $uv$ .
7:   end for
8:    $k \leftarrow 0$ .
9:   while a link remains do
10:    while there exists a link  $uv$  with  $c[uv] \leq k$  do
11:       $\ell[uv] \leftarrow k$ .
12:      for  $w \in \text{COMMONNEIGHBOR}(G', G, u, v)$  do
13:         $c[wu] \leftarrow c[wu] - 1$  and  $c[vw] \leftarrow c[vw] - 1$ .
14:      end for
15:      Remove the link  $uv$ , and update  $G$  and  $G'$ .
16:    end while
17:     $k \leftarrow k + 1$ .
18:  end while
19: end procedure
```

Algorithm 3

```
1: procedure FLOWTRUSS( $G$ ) ▷ Find flow-trusses in  $G$ 
2:   Let  $G'$  be the network obtained from  $G$  by reversing the directions of links.
3:    $c[e] \leftarrow 0$  for each  $e \in E(G)$ .
4:    $\ell[e] \leftarrow \infty$  for each  $e \in E(G)$ .
5:   for  $uv \in E(G)$  do
6:      $c[uv] \leftarrow |\text{COMMONNEIGHBOR}(G, G', u, v)|$ .
7:     ▷ Count flow triangles with links  $uv$ ,  $wv$ , and  $uw$  for some  $w \in V(G)$ .
8:      $c[uv] \leftarrow c[uv] + |\text{COMMONNEIGHBOR}(G', G', u, v)|$ .
9:     ▷ Count flow triangles with links  $uv$ ,  $wv$ , and  $wu$  for some  $w \in V(G)$ .
10:     $c[uv] \leftarrow c[uv] + |\text{COMMONNEIGHBOR}(G, G, u, v)|$ .
11:    ▷ Count flow triangles with links  $uv$ ,  $vw$ , and  $uw$  for some  $w \in V(G)$ .
12:  end for
13:   $k \leftarrow 0$ .
14:  while a link remains do
15:    while there exists a link  $uv$  with  $c[uv] \leq k$  do
16:       $\ell[uv] \leftarrow k$ .
17:      for  $w \in \text{COMMONNEIGHBOR}(G, G', u, v)$  do
18:         $c[uw] \leftarrow c[uw] - 1$  and  $c[wv] \leftarrow c[wv] - 1$ .
19:      end for
20:      for  $w \in \text{COMMONNEIGHBOR}(G', G', u, v)$  do
21:         $c[wu] \leftarrow c[wu] - 1$  and  $c[wv] \leftarrow c[wv] - 1$ .
22:      end for
23:      for  $w \in \text{COMMONNEIGHBOR}(G, G, u, v)$  do
24:         $c[wu] \leftarrow c[wu] - 1$  and  $c[vw] \leftarrow c[vw] - 1$ .
25:      end for
26:      Remove the link  $uv$ , and update  $G$  and  $G'$ .
27:    end while
28:     $k \leftarrow k + 1$ .
29:  end while
30: end procedure
```

Supplementary Materials

for

Taro Takaguchi and Yuichi Yoshida

Cycle and flow trusses in directed networks

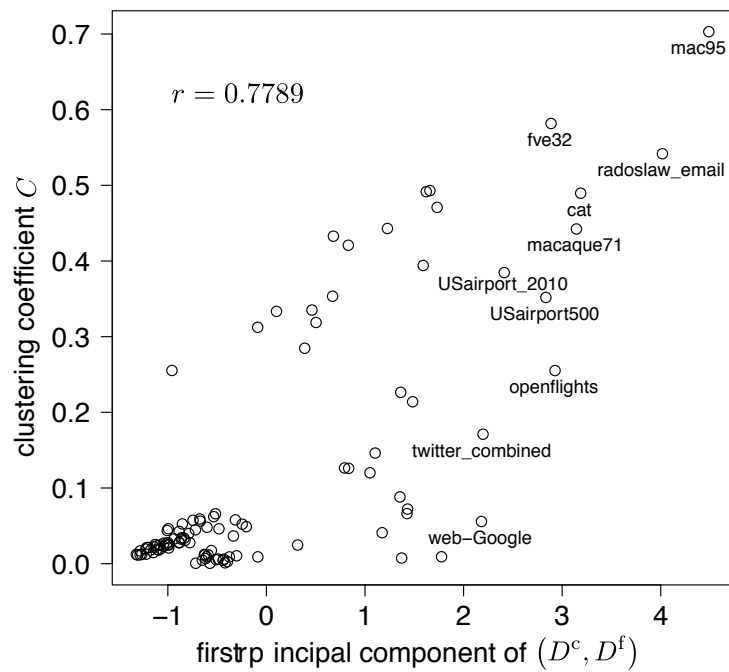


Figure S1: **Scatter plot of the values of the first principal component of (D^c, D^f) and the clustering coefficient for various networks.** The clustering coefficient is calculated with regarding networks as undirected. The points corresponding to the ten networks with the largest values of the principal component are indicated with the names of networks. The r value is the Pearson correlation coefficient.

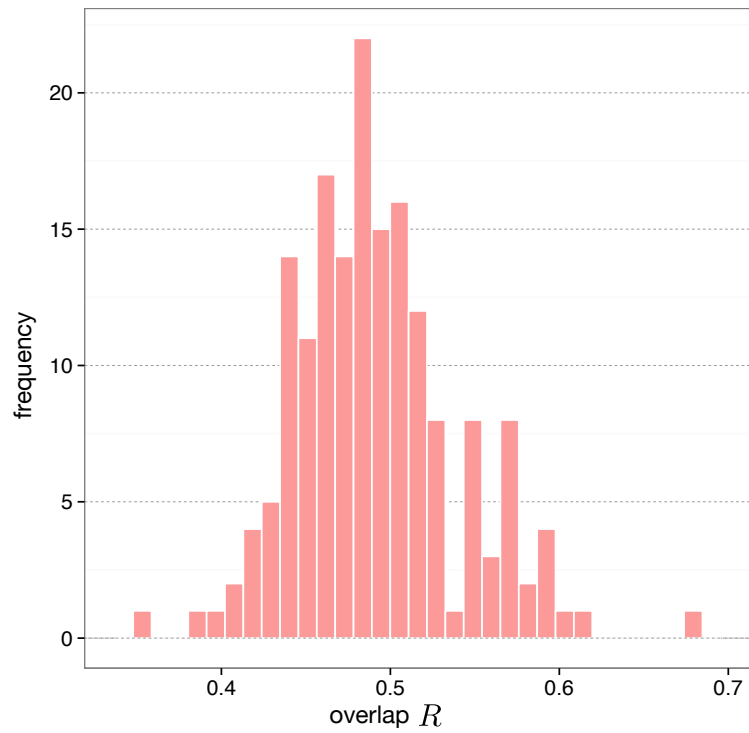


Figure S2: **Histogram of the R measure for the metabolic networks.** The measure R quantifies the overlap between the set of links with the largest k^c values and that with the largest k^f values.

Table S1: **Statistics of the empirical network used in this study.** N and M : the number of nodes and links. k_{\max}^c and k_{\max}^f : the maximum cycle and flow truss numbers. C : the average clustering coefficient after discarding the link direction. T^c and T^f : the number of the cycle and flow triangles. M^{bid} : the number of links whose node pairs have another link in the opposite direction.

name	N	M	k_{\max}^c	k_{\max}^f	C	T^c	T^f	M^{bid}
airport								
openflights [1]	2939	30501	21	63	0.2547	72631	72803	29648
USairport500 [2]	500	5960	25	75	0.3514	18424	18424	5960
USairport_2010 [3]	1574	28236	54	163	0.3841	220832	243384	22042
circuit								
s208_st [4]	122	189	1	0	0.0574	10	0	0
s420_st [4]	252	399	1	0	0.0517	20	0	0
s838_st [4]	512	819	1	0	0.0483	40	0	0
citation								
allcites [5,6]	25417	216738	1	13	0.1260	49	385667	564
cit-HepPh [7, 8]	34546	421534	1	23	0.1457	506	1276803	1314
cit-HepTh [7, 8]	27769	352768	3	28	0.1196	522	1478675	966
communication								
email-EuAll [9]	265009	418956	12	39	0.0041	134844	266308	108950
enron [10]	86978	320154	13	50	0.0716	255012	1171455	45396
munmun_digg_reply [11]	30360	85247	1	2	0.0056	286	4028	184
opsahl-ucsocial [12]	1899	20296	3	10	0.0568	8441	14253	12916
radoslaw_email [13]	168	11544	62	189	0.8246	176867	203312	9266
slashdot-threads [14]	51083	130370	2	5	0.0060	4320	18175	27594
wiki-Talk [15]	2394385	5021410	28	91	0.0022	4302222	9031616	723690
following								
munmun_twitter_social [16]	465017	834797	1	4	0.0006	119	38375	2514
polblogs [17]	1224	19022	9	32	0.2260	18481	100562	4614
soc-Epinions1 [18]	75879	508837	18	60	0.0657	580213	1616825	206194
soc-Slashdot0902 [19]	82168	870161	33	99	0.0241	493487	602500	731862
twitter_combined [20]	81306	1768135	41	139	0.1706	5118668	13059341	851678
wiki-Vote [21, 22]	7115	103689	6	25	0.1255	41856	601594	5854

Table S2: Statistics of the empirical network used in this study (continued).

name	N	M	k_{\max}^c	k_{\max}^f	C	T^c	T^f	M^{bid}
foodweb								
Chesapeake [23]	39	176	1	3	0.2842	14	194	12
ChesLower [24]	37	177	1	4	0.3529	24	241	20
ChesMiddle [24]	37	207	1	6	0.4323	38	383	18
ChesUpper [24]	37	214	1	5	0.4203	44	393	30
CrystalC [25, 26]	24	125	1	5	0.4925	41	209	22
CrystalD [25, 26]	24	99	1	4	0.3936	24	127	14
Everglades [27]	69	911	2	10	0.4704	536	4344	62
Florida [28]	128	2106	1	9	0.3119	357	8367	62
Maspalomas [29]	24	82	1	2	0.3182	9	59	10
Michigan [30]	39	218	1	4	0.3347	52	332	18
Mondego [31]	46	392	1	9	0.4911	224	1185	68
Narragan [32]	35	218	1	5	0.4425	69	446	28
Rhode [33]	19	53	0	2	0.2548	0	22	16
StMarks [34]	54	353	1	5	0.3329	15	650	6
gene								
Hs_Tr [35]	3107	6873	1	5	0.0084	46	2690	72
Mm_Tr [35]	1192	2393	1	2	0.0087	1	206	0
Mt_Tr [35]	755	887	0	2	0.0047	0	49	6
Rr_Tr [35]	533	1089	0	1	0.0118	0	102	6
Sc_Tr [35]	4441	12873	1	4	0.0099	13	3742	18
P2P								
p2p-Gnutella04 [9, 36]	10876	39994	1	2	0.0054	33	901	0
p2p-Gnutella31 [9, 36]	62586	147892	1	2	0.0039	57	1967	0
neural								
cat [37]	95	2126	8	25	0.4891	5367	5929	1912
celegans_neural [38]	279	2990	3	9	0.2135	1414	4408	1406
fve32 [39]	32	315	4	13	0.5812	380	486	242
macaque71 [40]	71	746	4	12	0.4418	813	957	616
mac95 [41, 42]	94	2390	15	47	0.7926	9145	13802	1750
software								
subelj_jdk [43]	6434	53892	2	16	0.0111	288	194798	468
subelj_jung-j [43]	6210	50535	4	16	0.0110	300	182009	490
web								
web-BerkStan [19]	685224	7600545	161	483	0.0069	7426999	64666756	1902224
web-Google [19]	875713	5105039	31	93	0.0552	2486567	13357485	1565976
web-NotreDame [44]	325729	1469679	148	444	0.0877	6936636	8900531	759142
web-Stanford [19]	281903	2312497	40	120	0.0086	689426	11320457	639722
word								
darwinbookinter_st [45]	7381	46281	7	22	0.0361	63392	144954	4148
Edinburgh Associative Thesaurus [46]	23132	311758	2	8	0.0404	49884	395238	29328
frenchbookinter_st [45]	8325	24295	3	7	0.0118	6543	15834	908
japanesebookinter_st [45]	2704	8300	3	9	0.0301	3194	7320	604
lasagne-spanishbook [43]	12643	57451	5	21	0.0085	47110	110228	4864
lasagne-yahoo [43]	653260	2931706	1	1	5.2×10^{-6}	4	67256	16
spanishbookinter_st [45]	11586	45129	5	21	0.0168	40868	97112	4128

References

- [1] T. Opsahl, F. Agneessens, J. Skvoretz. Node centrality in weighted networks: Generalizing degree and shortest paths. *Soc. Networks* **32**, 245–251 (2010).
- [2] V. Colizza, R. Pastor-Satorras, A. Vespignani. Reaction-diffusion processes and metapopulation models in heterogeneous networks. *Nat. Phys.* **3**, 276–282 (2007).
- [3] Tore Opsahl. Why Anchorage is not (that) important: Binary ties and Sample selection, <http://toreopsahl.com/2011/08/12/why-anchorage-is-not-that-important-binary-ties-and-sample-selection/> (Date accessed: 1st March 2016).
- [4] R. Milo, S. Shen-Orr, S. Itzkovitz, N. Kashtan, D. Chklovskii, U. Alon. Network motifs: simple building blocks of complex networks. *Science (New York, N.Y.)* **298**, 824–827 (2002).
- [5] J. H. Fowler, T. R. Johnson, J. F. Spriggs, S. Jeon, P. J. Wahlbeck. Network analysis and the law: Measuring the legal importance of precedents at the U.S. supreme court. *Polit. Anal.* **15**, 324–346 (2007).
- [6] J. H. Fowler, S. Jeon. The authority of Supreme Court precedent. *Soc. Networks* **30**, 16–30 (2008).
- [7] J. Gehrke, P. Ginsparg, J. Kleinberg. Overview of the 2003 KDD Cup. *ACM SIGKDD Explor.* **5**, 149 (2003).
- [8] J. Leskovec, J. Kleinberg, C. Faloutsos. Graphs over time: Densification laws, shrinking diameters and possible explanations. *Proceedings of the eleventh ACM SIGKDD international conference on Knowledge discovery in data mining*, Chicago, IL, USA, 21 to 24 August 2005, pp. 177–187.

- [9] J. Leskovec, J. Kleinberg, C. Faloutsos. Graph evolution: Densification and shrinking diameters. *ACM Trans. Knowl. Discov. Data* **1**, 2 (2007).
- [10] B. Klimt, Y. Yang. The Enron corpus: A new dataset for email classification research. *Proceedings of 15th European Conference on Machine Learning*, Pisa, Italy, 20 to 24 September 2004, pp. 217–226.
- [11] M. De Choudhury, H. Sundaram, A. John, D. D. Seligmann. Social synchrony: Predicting mimicry of user actions in online social media. *Proceedings of International Conference on Computational Science and Engineering* **4**, Vancouver, BC, Canada, 29 to 31 August 2009, pp. 151–158.
- [12] T. Opsahl, P. Panzarasa. Clustering in weighted networks. *Soc. Networks* **31**, 155–163 (2009).
- [13] R. Michalski, S. Palus, P. Kazienko. Matching organizational structure and social network extracted from email communication. *Proceedings of 14th International Conference on Business Information Systems*, Pożan, Poland, 15 to 17 June 2011, pp. 197–206.
- [14] V. Gómez, A. Kaltenbrunner, V. López. Statistical analysis of the social network and discussion threads in slashdot. *Proceedings of the 17th international conference on World Wide Web*, Beijing, China, 21 to 25 April 2008, pp. 645–654.
- [15] J. Leskovec, D. P. Huttenlocher, J. M. Kleinberg. Governance in social media: A case study of the Wikipedia promotion process. *Proceedings of Fourth International AAAI Conference on Weblogs and Social Media*, Washington, D.C., USA, 23 to 26 May 2010, pp. 98–105.
- [16] M. De Choudhury, Y.-R. Lin, H. Sundaram, K. S. Candan, L. Xie, A. Kelliher. How does the data sampling strategy impact the discovery of information diffusion in social media? *Proceedings of Fourth International AAAI Conference on Weblogs and Social Media*, Washington, D.C., USA, 23 to 26 May 2010, pp. 34–41.

- [17] L. A. Adamic, N. Glance. The political blogosphere and the 2004 US election: divided they blog. *Proceedings of the 3rd international workshop on Link discovery*, Chicago, IL, USA, 21 to 24 August 2005, pp. 36–43.
- [18] M. Richardson, R. Agrawal, P. Domingos. Trust management for the semantic web. *Proceedings of the Second International Semantic Web Conference*, Sanibel Island, FL, USA, 20 to 23 October 2003, pp. 351–368.
- [19] J. Leskovec, K.J. Lang, A. Dasgupta, M.W. Mahoney. Community structure in large networks: Natural cluster sizes and the absence of large well-defined clusters. *Internet Math.* **6**, 29–123 (2009).
- [20] J. Mcauley, J. Leskovec. Discovering social circles in ego networks. *ACM Trans. Knowl. Discov. Data* **8**, 1–28 (2014).
- [21] J. Leskovec, D. Huttenlocher, J. Kleinberg. Signed networks in social media. *Proceedings of the SIGCHI Conference on Human Factors in Computing Systems*, Atlanta, GA, USA, 10 to 15 April 2010, pp. 1361–1370.
- [22] J. Leskovec, D. Huttenlocher, J. Kleinberg. Predicting positive and negative links in online social networks. *Proceedings of the 19th international conference on World wide web*, Raleigh, NC, USA, 26 to 30 April 2010, pp. 641–650.
- [23] D. Baird, R. E. Ulanowicz. The seasonal dynamics of the Chesapeake Bay ecosystem. *Ecol. Monogr.* **59**, 329 (1989).
- [24] J. D. Hagy. *Eutrophication, hypoxia and trophic transfer efficiency in Chesapeake Bay*. PhD thesis, University of Maryland, 2002.
- [25] M. Homer, W. M. Kemp. unpublished manuscript.
- [26] R. E. Ulanowicz. *Growth and Development: Ecosystems Phenomenology*. (Springer New York, New York, NY, 1986).

- [27] R. E. Ulanowicz, J. J. Heymans, M. S. Egnotoivich. Network analysis of trophic dynamics in south Florida ecosystems, FY 99: The Graminoid ecosystem. Technical report, Center for Environmental Science, the University of Maryland, Solomons, MD, 2000.
- [28] R. E. Ulanowicz, C. Bondavalli, M. S. Egnotovich. Network analysis of trophic dynamics in south Florida ecosystem, FY 97: The Florida Bay ecosystem. Technical report, Chesapeake Biological Laboratory, University of Maryland, Solomons, MD, 1998.
- [29] J. Almunia, G. Basterretxea, J. Arístegui, R. E. Ulanowicz. Benthic-pelagic switching in a coastal subtropical lagoon. *Estuar. Coast. Shelf Sci.* **49**, 363–384 (1999).
- [30] A. E. Krause. *The role of compartments in food-web structure and changes following biological invasions in southeast Lake Michigan*. Ph.D thesis, Michigan State University, 2004.
- [31] J. Patricio. Master’s thesis, University of Coimbra, Portugal, 2002.
- [32] M. E. Monaco and R. E. Ulanowicz. Comparative ecosystem trophic structure of three U.S. mid-Atlantic estuaries. *Mar. Ecol. Prog. Ser.* **161**, 239–254 (1997).
- [33] D. Correll. unpublished manuscript.
- [34] D. Baird, J Luczkovich, R. R. Christian. Assessment of spatial and temporal variability in ecosystem attributes of the St Marks national wildlife refuge, Apalachee Bay, Florida. *Estuar. Coast. Shelf Sci.* **47**, 329–349 (1998).
- [35] N. Bhardwaj, K.-K. Yan, M. B. Gerstein. Analysis of diverse regulatory networks in a hierarchical context shows consistent tendencies for collaboration in the middle levels. *Proc. Natl. Acad. Sci. U.S.A.* **107**, 6841–6846 (2010).
- [36] M. Ripeanu, I. Foster. Mapping the Gnutella network: Macroscopic properties of large-scale peer-to-peer systems. *IEEE Internet Comput. J.*, 6, (2002).

- [37] J. W. Scannell, G. A. P. C. Burns, C. C. Hilgetag, M. A. O’Neil, M. P. Young. The connectional organization of the cortico-thalamic system of the cat. *Cereb. Cortex* **9**, 277–299 (1999).
- [38] L. R. Varshney, B. L. Chen, E. Paniagua, D. H. Hall, D. B. Chklovskii. Structural properties of the *Caenorhabditis elegans* neuronal network. *PLOS Comput. Biol.* **7**, e1001066 (2011).
- [39] D. J. Felleman, D. C. Van Essen. Distributed hierarchical processing in the primate cerebral cortex. *Cereb. Cortex* **1**, 1–47 (1991).
- [40] M. P. Young. The organization of neural systems in the primate cerebral cortex. *Proc. R. Soc. B* **252**, 13–18 (1993).
- [41] M. Kaiser, C. C. Hilgetag. Nonoptimal component placement, but short processing paths, due to long-distance projections in neural systems. *PLOS Comput. Biol.* **2**, e95 (2006).
- [42] R. Kötter. Online retrieval, processing, and visualization of primate connectivity data from the CoCoMac database. *Neuroinformatics* **2**, 27–144 (2004).
- [43] KONECT: the Koblenz Network Collection. <http://konect.uni-koblenz.de/> (Date accessed: 1st March 2016).
- [44] R. Albert, A.-L. Barabási, H. Jeong. Diameter of the World-Wide Web. *Nature* **401**, 130–131 (1999).
- [45] R. Milo, S. Itzkovitz, N. Kashtan, R. Levitt, S. Shen-Orr, I. Ayzenshtat, M. Sheffer, U. Alon. Superfamilies of evolved and designed networks. *Science (New York, N.Y.)* **303**, 1538–1542 (2004).
- [46] G. R. Kiss, C. Armstrong, R. Milroy, J. Piper. An associative thesaurus of English and its computer analysis. In *The computer and literary studies*, A.J. Aitken, R.W. Bailey, N. Hamilton-Smith, Eds. (Edinburgh University Press, 1973), pp. 153–165.